

# Spin-orbit ab initio study of two low-lying states of chloroiodomethane cation

Joonghan Kim · Hyotcherl Ihée · Yoon Sup Lee

Received: 8 October 2010 / Accepted: 27 October 2010 / Published online: 12 November 2010  
© Springer-Verlag 2010

**Abstract** Spin-orbit coupling plays a crucial role in the determination of molecular structure and calculation of vibrational frequencies of  $\text{CH}_2\text{ClI}^+$ . We performed the geometry optimizations and vibrational frequency calculations of both the lower and upper spin-orbit (SO) states using an ab initio SO method based on multiconfigurational wave function. The multistate complete active space perturbation theory second-order SO (MS-CASPT2-SO) method reasonably describes the structures of the lower SO state, yielding the C–I distance and the I–C–Cl angle close to the experimental values. The geometrical parameters of the upper SO state is quite similar to that of the lower SO state, whereas structures of two states differ substantially in calculations prior to the introduction of SO coupling. The MS-CASPT2-SO method reproduces the difference between the lower and upper SO states for the I–C–Cl bending frequency. The vibrational frequencies calculated by MS-CASPT2-SO generally overestimate in comparison with the experiments. The energy gap between the two SO states calculated by MS-CASPT2-SO is reasonably close to the experimental value. To the best of our knowledge, this

is the first attempt to calculate vibrational frequencies of two SO states of  $\text{CH}_2\text{ClI}^+$ , and the first time to apply MS-CASPT2-SO method to the geometry optimization and vibrational frequency calculation of polyatomic molecule.

**Keywords** Dihalomethane · Cation · Spin-orbit coupling · Ab initio

## 1 Introduction

Halomethanes have served as a long-standing prototypical molecular system for experimental and theoretical chemists, since they are highly related to environmental issues [1, 2] and useful for the understanding of photochemical reaction mechanism. Accordingly, numerous theoretical [3–11] and experimental [12–17] studies have been undertaken to elucidate their electronic structure and photodynamical characters. In addition, when a halomethane contains heavy halogen atom such as Br and I, the spin-orbit coupling (SOC) may play a key role in the interpretation of experimental results.

Recent investigation has shown that the molecular geometries and vibrational frequencies of dihalomethane cation are strongly affected by SOC [18–20]. The importance of SOC, which is one of relativistic effect [21], is demonstrated when the lower spin-orbit (SO) state of  $\text{CH}_2\text{ClI}^+$  is correctly elucidated by the two-component spin-orbit density functional theory (SODFT) [22] with the relativistic effective core potential (RECP) [18, 19] only upon the inclusion of SO terms. Especially, the bending frequency of the I–C–Cl angle calculated by SODFT is close to the experimental value. However, both the SODFT and the time-dependent DFT (TDDFT) did not locate the upper SO state, which may be considered as an SO excited state [23].

---

This paper is dedicated to Prof. Pekka Pyykkö, on the occasion of his 70th birthday, in recognition of his great contributions to theoretical chemistry and published as part of the Pyykkö Festschrift Issue.

J. Kim · H. Ihée  
Center for Time-Resolved Diffraction, Department of Chemistry, Graduate School of Nanoscience & Technology (WCU), KAIST, Daejeon 305-701, Republic of Korea

J. Kim · Y. S. Lee (✉)  
Department of Chemistry, KAIST, Daejeon 305-701,  
Republic of Korea  
e-mail: yslee@kaist.edu

Two-component SCF methods like Hartree–Fock (HF) and DFT methods using the RECP well describe the SOC in a cost-effective manner but are limited in treating the SO excited state. In contrast, the SO ab initio methods based on a multiconfigurational approach [24, 25] reasonably work in calculations of the excited states as well as the ground states, but additional work is required for geometry optimization and vibrational frequency calculation due to the lack of the analytical gradient. Thus, the latter method has been mainly used for simple diatomic molecules to calculate the potential energy surfaces (PESs) [26, 27] and for halomethanes to calculate PES along the dissociation coordinate [4, 5, 9, 10]. Both approaches provide reasonable results for the calculations of SO states. Since the gradients and hessians can be calculated numerically for small polyatomic molecules, geometry optimizations and vibration frequency calculations are possible for all SO states using the latter method. The SO effect on the molecular structure and the shape of PES for the SO ground state as well as the excited states can be identified through this method.  $\text{CH}_2\text{ClI}^+$  is an appropriate molecule for this purpose. Moreover, the experimental results [18, 19, 23] of  $\text{CH}_2\text{ClI}^+$  are available, so that they can be used to assess the performance of the ab initio SO method based on a multiconfigurational wave function for the geometry optimizations and vibrational frequency calculations.

In the present work, we have applied the ab initio SO method to two SO states of  $\text{CH}_2\text{ClI}^+$ , where a large SO effect arises. The geometries of both SO lower and upper states are optimized and the vibrational frequencies are also calculated, and the results are compared with available experimental results.

## 2 Computational details

The complete active space self-consistent field (CASSCF) [28] method was used to obtain the wave functions of  ${}^2\text{A}'$  and  ${}^2\text{A}''$  states of  $\text{CH}_2\text{ClI}^+$ . In the CASSCF calculations, eleven electrons were distributed in ten active orbitals (CAS(11,10)) for  $\text{CH}_2\text{ClI}^+$ . The active orbitals contain  $\sigma$  bonding orbitals of C–I and C–Cl,  $\sigma^*$  antibonding orbitals of C–I and C–Cl, and nonbonding orbitals (p orbitals) of I and Cl. The scalar relativistic effects were considered using the second-order Douglas–Kroll–Hess (DKH2) method [29, 30]. The ANO-RCC [31] all-electron basis sets were used for all atoms (C, (14s9p4d)/[4s3p2d]; H, (8s4p3d)/[3s2p1d]; Cl, (17s12p5d4f)/[5s4p2d1f]; I, (22s19p13d5f)/[7s6p4d3f]). We used  $C_1$  symmetry instead of  $C_s$  symmetry, so that both  $\text{A}'$  and  $\text{A}''$  states can be calculated simultaneously using the state-average CASSCF (SA-CASSCF). Subsequently, the multistate multiconfigurational second-order perturbation

theory (MS-CASPT2) [32] was used to consider the dynamic electron correlation effect. The SO coupled states were calculated using the restricted active space state interaction with spin–orbit coupling (RASSI-SO) [25] method with the atomic mean field integrals (AMFI) for SOC [33]. In SO calculations, an effective one-electron Fock-type SO Hamiltonian was used [33]. All SO coupled states of  $\text{CH}_2\text{ClI}^+$  were obtained by a diagonalization of four spin-free states,  ${}^2\text{A}'$ ,  ${}^2\text{A}''$ ,  ${}^4\text{A}'$ , and  ${}^4\text{A}''$ . Through these processes, we can obtain the electronic energies of the lower and upper SO states of  $\text{CH}_2\text{ClI}^+$ . The Molcas6.4 program [34] was used to obtain the electronic energies of the SO states and to optimize the geometries of two spin-free states,  ${}^2\text{A}'$  and  ${}^2\text{A}''$ .

For the geometry optimizations, we developed our own code. The Cartesian numerical gradients were calculated using the electronic energies of the SO coupled states obtained from the Molcas6.4 program [34]. We used the central difference formula for the evaluation of the numerical gradients. The central difference formula is given by

$$\frac{\partial E}{\partial x_i} \approx \frac{1}{2h} [E(x_i + h) - E(x_i - h)] \quad (1)$$

where  $x_i$  and  $h$  are the Cartesian nuclear coordinate and displacement, respectively. The steepest descent algorithm was used for the geometry optimizations. We used one-fifth of the default values of convergence criteria in usual quantum chemical programs as the criteria for the geometry optimizations (maximum force, 0.000090 (hartree/bohr); root-mean-square force, 0.000060 (hartree/bohr); maximum displacement, 0.000360 (bohr); root-mean-square displacement, 0.000240 (bohr)).

We calculated the Cartesian numerical hessians on the optimized geometries to obtain the vibrational frequencies of the SO states of  $\text{CH}_2\text{ClI}^+$ . The numerical hessians were evaluated using the following formulas:

$$\frac{\partial^2 E}{\partial x_i \partial x_j} \approx \frac{1}{h^2} [E(x_i - h, x_j) - 2E(x_i, x_j) + E(x_i + h, x_j)] \quad \text{for } i = j \quad (2)$$

$$\begin{aligned} \frac{\partial^2 E}{\partial x_i \partial x_j} \approx & \frac{1}{4h^2} [E(x_i - h, x_j - h) - E(x_i + h, x_j - h) \\ & - E(x_i - h, x_j + h) + E(x_i + h, x_j + h)] \quad \text{for } i \neq j \end{aligned} \quad (3)$$

The optimal value of the displacement was 0.025 Å for the geometry optimizations and vibrational frequency calculations. A total of fifteen Cartesian nuclear coordinates were used for  $\text{CH}_2\text{ClI}^+$ . We also calculated the harmonic vibrational frequencies of the SO states of  $\text{CH}_2\text{ClI}^+$  using our own code.

### 3 Results and discussion

$\text{CH}_2\text{ClI}^+$  has been generated through a removal of one electron from neutral  $\text{CH}_2\text{ClI}$ . Thus,  $^2\text{A}'$  or  $^2\text{A}''$  electronic states appear as an unpaired electron occupying  $a'$  or  $a''$  orbitals, respectively, in the absence of SOC. In the presence of SOC, SOC mixes both  $^2\text{A}'$  and  $^2\text{A}''$ , and then generates the lower and upper SO states. These phenomena are well explained through simple single-point calculations. We have performed the single-point calculations with the varying Cl–C–I angle, and the calculated results are depicted in Fig. 1. SOC increases the energy gap between  $^2\text{A}'$  and  $^2\text{A}''$  as if the two states repelled each other. Since both states belong to the same symmetry ( $^2\text{E}_{1/2}$ ) in the double group symmetry, the energy gap increases in the presence of SOC. We note that the minimum points and shapes of PESs of the lower and upper SO states are considerably different from those of  $^2\text{A}'$  and  $^2\text{A}''$  states. SOC strongly affects the molecular geometries and the vibrational frequencies, which are related to the shape of the PES.

To identify the optimized geometrical parameters of  $\text{CH}_2\text{ClI}^+$  in the absence of SOC, we performed geometry optimizations for  $^2\text{A}'$  and  $^2\text{A}''$  states using SA-CASSCF and MS-CASPT2, and the results are summarized in Table 1. As can be seen in Table 1, MS-CASPT2 reasonably

reproduces the geometrical characters of  $^2\text{A}'$  and  $^2\text{A}''$  states of previous B3LYP calculations [19]. For example, the C–I distance of the  $^2\text{A}'$  state is shorter than that of the  $^2\text{A}''$  state, and MS-CASPT2 results also follow this trend. However, MS-CASPT2 gives the shorter C–I distance than that of B3LYP. This trend of the C–I bond length was also reported for  $\text{CF}_2\text{ICF}_2\text{I}$  [35]. The I–C–Cl angles for  $^2\text{A}'$  and  $^2\text{A}''$  states calculated by MS-CASPT2 are similar to those calculated by B3LYP. From the difference between SA-CASSCF (104.8°) and MS-CASPT2 (94.3°) I–C–Cl angles, it is apparent that the I–C–Cl angle of the  $^2\text{A}'$  state sensitively changes by the dynamic electron correlation effect. In all other geometrical parameters, the results of MS-CASPT2 are acceptably close to those of B3LYP. From these results of the spin-free calculations, we conclude that the size of basis sets and the selection of the active orbitals are appropriate for the MS-CASPT2 calculations.

To examine the SO effect on the molecular geometries of  $\text{CH}_2\text{ClI}^+$ , we have performed the geometry optimizations of the lower and upper SO states and the calculated results are summarized in Table 2. The lower SO state is composed of 55.1% of  $^2\text{A}'$ , 44.7% of  $^2\text{A}''$ , 0.1% of  $^4\text{A}'$ , and 0.1% of  $^4\text{A}''$  state. The upper SO state is composed of 46.5% of  $^2\text{A}'$  state, 53.4% of  $^2\text{A}''$ , and 0.1% of  $^4\text{A}''$ . Due to the similar contributions of the spin-free states, similar equilibrium geometries are expected for the SO-coupled

**Fig. 1** **a** PESs of  $\text{CH}_2\text{ClI}^+$  calculated by MS-CASPT2. **b** PESs of  $\text{CH}_2\text{ClI}^+$  calculated by MS-CASPT2-SO

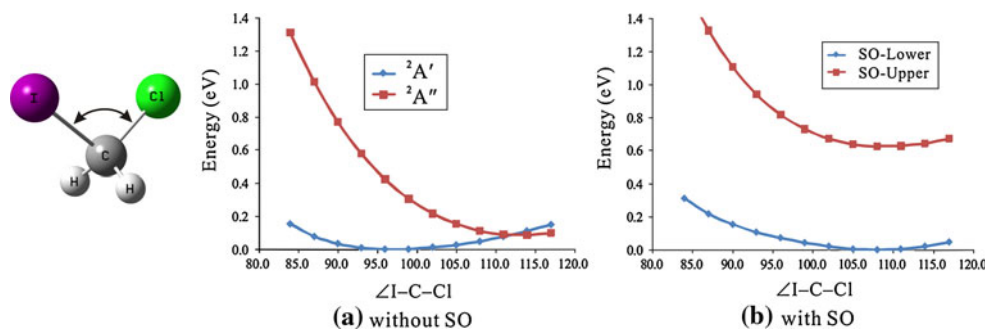


**Table 1** Optimized geometrical parameters of  $\text{CH}_2\text{ClI}^+$  of  $^2\text{A}'$  and  $^2\text{A}''$  calculated by SA-CASSCF and MS-CASPT2

w/o SO	$^2\text{A}'$			$^2\text{A}''$		
	SA-CAS(11,10)	MS-CASPT2	B3LYP <sup>a</sup>	SA-CAS(11,10)	MS-CASPT2	B3LYP <sup>a</sup>
C–I	2.277	2.157	2.187	2.307	2.223	2.243
C–Cl	1.740	1.757	1.767	1.721	1.710	1.716
C–H	1.069	1.075	1.082	1.071	1.081	1.090
$\angle\text{ICCI}$	104.8	94.3	96.1	112.3	113.5	116.1
$\angle\text{ICH}$	104.0	109.1	109.6	100.3	100.6	101.0
$\angle\text{CICH}$	113.0	112.6	111.9	113.7	113.8	112.9
$\angle\text{HCH}$	116.4	116.7	115.8	114.9	113.0	111.8

<sup>a</sup> Reference [19]

**Table 2** Optimized geometrical parameters and vibrational frequencies of the SO lower and upper states of  $\text{CH}_2\text{ClI}^+$  calculated by MS-CASPT2-SO

With SO	SO Lower			SO Upper	
	MS-CASPT2-SO	SODFT <sup>a</sup> (B3LYP)	Exp. <sup>a,b</sup>	MS-CASPT2-SO	Exp. <sup>c</sup>
C–I	2.217	2.242	$2.191 \pm 0.003$	2.223	—
C–Cl	1.723	1.738	$1.745 \pm 0.002$	1.719	—
C–H	1.078	1.084	—	1.079	—
$\angle\text{ICCI}$	108.0	106.0	$107.09 \pm 0.09$	109.0	—
$\angle\text{ICH}$	103.1	104.9	$106.43 \pm 0.12$	102.5	—
$\angle\text{CICH}$	113.3	112.7	—	113.5	—
$\angle\text{HCH}$	114.6	114.5	—	114.5	—
C–H symm. stretch	3,144	3,106	—	3,136	—
CH <sub>2</sub> scissoring	1,436	1,420	1,385	1,431	1,398
CH <sub>2</sub> wagging	1,208	1,175	1,164	1,204	1,133
C–Cl stretch	781	747	767	786	793
C–I stretch	422	419	408	422	371
I–C–Cl bending	131	112	114	161	144
C–H asymm. stretch	3,247	3,206	—	3,237	—
CH <sub>2</sub> twisting	1,086	1,089	1,072	1,066	—
CH <sub>2</sub> rocking	779	791	—	748	—

<sup>a</sup> Reference [19]<sup>b</sup> Reference [18]<sup>c</sup> Reference [23]

states. The MS-CASPT2-SO method reasonably describes the characters of the lower SO state, in particular the I–C–Cl angle. Spectral fitting result for the I–C–Cl angle is  $107.09 \pm 0.09$  [20], and the DFT and MS-CASPT2 cannot provide correct results for the I–C–Cl angle without considering SOC. On the other hand, the MS-CASPT2-SO method gives correct result ( $108.0^\circ$ ) for the I–C–Cl angle, in good agreement with the experimental value. MS-CASPT2-SO slightly overestimates and underestimates the C–I and C–Cl bond lengths, respectively. However, in the C–I distance, MS-CASPT2-SO method gives better results than SODFT. The geometrical parameters of the lower SO state calculated by MS-CASPT2-SO are generally similar to those calculated by SODFT. In the case of the upper SO state, there exist neither experimental nor calculated values for the molecular structure. We expect that the MS-CASPT2-SO method would also provide reasonable description of the upper SO state of  $\text{CH}_2\text{ClI}^+$ , because the lower SO state is accurately described by the MS-CASPT2-SO method. As shown in Table 2, the optimized molecular structure of the upper SO state is similar to that of the lower SO state. The C–I distance of the upper SO state is slightly longer than that of the lower SO state, whereas the opposite result is obtained for the C–Cl distance. The I–C–Cl and I–C–H angles of the upper SO state are slightly larger and smaller than those of the lower SO state,

respectively. Other geometrical parameters of the upper SO state are quite similar to those of the lower SO state.

We have performed the harmonic vibrational frequency calculations on the optimized structures of the lower and upper SO states and the results are summarized in Table 2. As can be seen in Table 2, MS-CASPT2-SO slightly overestimates the vibrational frequencies for the lower SO state compared with the experimental values. The results for the lower SO state calculated by SODFT are generally closer to the experiment, but in some values such as the C–Cl stretching and CH<sub>2</sub> twisting frequencies, MS-CASPT2-SO provides better results than SODFT. In the upper SO state, MS-CASPT2-SO overestimates the vibrational frequencies but reproduces the trend between the lower and upper SO state for the I–C–Cl bending frequency. The experimental value for the I–C–Cl bending frequency of the lower SO state ( $114 \text{ cm}^{-1}$ ) is smaller than that of the upper SO state ( $144 \text{ cm}^{-1}$ ). The calculated results by MS-CASPT2-SO follow this trend well, and the difference ( $161 - 131 = 30 \text{ cm}^{-1}$ ) is in excellent agreement with the experiment ( $144 - 114 = 30 \text{ cm}^{-1}$ ). In all other frequencies, calculated frequencies for the two SO states are much closer than those of experiments. The source for this discrepancy is not clear at the moment. Some error might have been caused by numerical evaluation of the gradients and Hessians and even more errors by incomplete treatment of

higher-order SO and electron correlation effects. Since the MS-CASPT2-SO method overestimates the vibrational frequencies for all modes of the lower SO state as shown in Table 2, employing a proper scale factor would improve the overall agreement with the experimental values. This adjustment still would not change the closeness between calculated frequencies of the two SO states compared with experimental ones.

The energy gap between the two SO states calculated by MS-CASPT2-SO is 0.6229 eV. This value is reasonably close to that of experiment ( $0.5539 \pm 0.0012$  eV) [23] obtained by MATI spectrometry. We might conclude that MS-CASPT2-SO method of the present study also effectively describes the energetics induced by SOC.

To the best of our knowledge, this is the first time to apply MS-CASPT2-SO method to the geometry optimization and vibrational frequency calculation of polyatomic molecule. This method can also be applied to determine molecular structures and vibrational frequencies of other polyatomic molecules, where SOC plays a crucial role.

#### 4 Conclusions

The molecular structures and vibrational frequencies of both lower and upper SO states of  $\text{CH}_2\text{Cl}^+$  are calculated using the MS-CASPT2-SO method. The two states are structurally very similar since both of them have almost equal contributions of two spin-free states  $1^2\text{A}'$  and  $1^2\text{A}''$ . MS-CASPT2-SO calculations reasonably describe the characters of the lower SO state and gives the results that are similar to the previous SODFT results. For the C–I distance, MS-CASPT2-SO provides better results than SODFT. MS-CASPT2-SO reproduces the difference between the lower and upper SO state for the I–C–Cl bending frequency. The vibrational frequencies calculated by MS-CASPT2-SO are generally overestimated. The energy gap between the two SO states calculated by MS-CASPT2-SO is reasonably close to the experimental value. The MS-CASPT2-SO method seems to effectively work in the determination of the molecular structure, calculation of the vibrational frequency, and estimation of the energy gap between two SO states of  $\text{CH}_2\text{Cl}^+$ . We hope that this method applies to other molecular systems where SOC plays a crucial role in calculations of molecular properties.

**Acknowledgments** The authors thank Prof. M. S. Kim for helpful discussion and suggestion for this study. This work was supported by grants (2009-0084918, 2010-0001632) from National Research Foundation. Computational resources were provided by the supercomputing center of the Korea Institute of Science and Technology Information (KSC-2009-S02-0015). JK and HI acknowledge the support from Creative Research Initiatives (Center for Time-Resolved Diffraction) of MEST/NRF and the WCU program.

#### References

1. Aliche B, Hebestreit K, Stutz J, Platt U (1999) *Nature* 397:572–573
2. Finalayson-Pitts BJ, Pitts JN Jr (2000) *Chemistry of the upper and lower atmosphere*. Academic Press, San Diego
3. Ajitha D, Fedorov DG, Finley JP, Hirao K (2002) *J Chem Phys* 117:7068–7076
4. Ajitha D, Wierzbowska M, Lindh R, Malmqvist PA (2004) *J Chem Phys* 121:5761–5766
5. Alekseyev AB, Liebermann HP, Buenker RJ (2007) *J Chem Phys* 126:234102
6. Alekseyev AB, Liebermann HP, Buenker RJ (2007) *J Chem Phys* 126:234103
7. Amatatsu Y, Morokuma K, Yabushita S (1991) *J Chem Phys* 94:4858–4876
8. Amatatsu Y, Yabushita S, Morokuma K (1996) *J Chem Phys* 104:9783–9794
9. Liu YJ, Ajitha D, Krogh JW, Tarnovsky AN, Lindh R (2006) *Chem Phys Chem* 7:955–963
10. Liu YJ, Xiao HY, Sun MT, Fang WH (2008) *J Comput Chem* 29:2513–2519
11. Yabushita S, Morokuma K (1988) *Chem Phys Lett* 153:517–521
12. Eppink ATJB, Parker DH (1998) *J Chem Phys* 109:4758–4767
13. Eppink ATJB, Parker DH (1999) *J Chem Phys* 110:832–844
14. Gougousi T, Samartzis PC, Kitsopoulos TN (1998) *J Chem Phys* 108:5742–5746
15. Kim TK, Lee KW, Lee KS, Lee EK, Jung KH (2007) *Chem Phys Lett* 446:31–35
16. Kim TK, Park MS, Lee KW, Jung KH (2001) *J Chem Phys* 115:10745–10752
17. Kim YS, Kang WK, Jung KH (1996) *J Chem Phys* 105:551–557
18. Lee M, Kim H, Lee YS, Kim MS (2005) *J Chem Phys* 122:244319
19. Lee M, Kim H, Lee YS, Kim MS (2005) *Angew Chem Int Ed* 44: 2929–2931
20. Lee M, Kim H, Lee YS, Kim MS (2005) *J Chem Phys* 123: 024310
21. Pyykkö P (1988) *Chem Rev* 88:563–594
22. Nichols P, Govind N, Bylaska EJ, de Jong WA (2009) *J Chem Theory Comput* 5:491–499
23. Lee M, Kim MS (2006) *Chem Phys Lett* 431:19–23
24. Fedorov DG, Finley JP (2001) *Phys Rev A* 64:042502
25. Malmqvist PA, Roos BO, Schimmelpfennig B (2002) *Chem Phys Lett* 357:230–240
26. Ellingsen K, Saue T, Pouchan C, Gropen O (2005) *Chem Phys* 311:35–44
27. Gagliardi L, Roos BO (2005) *Nature* 433:848–851
28. Roos BO (1987) *Advances in chemical physics; ab initio methods in quantum chemistry II*. John Wiley and Sons, Chichester, England, p 399
29. Hess BA (1986) *Phys Rev A* 33:3742–3748
30. Jansen G, Hess BA (1989) *Phys Rev A* 39:6016–6017
31. Roos BO, Lindh R, Malmqvist PA, Veryazov V, Widmark PO (2004) *J Phys Chem A* 108:2851–2858
32. Finley J, Malmqvist PA, Roos BO, Serrano-Andres L (1998) *Chem Phys Lett* 288:299–306
33. Hess BA, Marian CM, Wahlgren U, Gropen O (1996) *Chem Phys Lett* 251:365–371
34. Karlstrom G, Lindh R, Malmqvist PA, Roos BO, Ryde U, Veryazov V, Widmark PO, Cossi M, Schimmelpfennig B, Neogrady P, Seijo L (2003) MOLCAS: a program package for computational chemistry. *Comput Mater Sci* 28:222–239
35. Kim J, Jun S, Kim J, Ihhee H (2009) *J Phys Chem A* 113: 11059–11066